Macromolecular Research, Vol. 15, No. 6, pp 553-559 (2007)

Synthesis and Characterization of Nanocomposite Films Consisting of Vanadium Oxide and Microphase-separated Graft Copolymer

Jin Kyu Choi, Yong Woo Kim, Joo Hwan Koh, and Jong Hak Kim*

Department of Chemical Engineering, Yonsei University, Seoul 120-749, Korea

Anne M. Mayes

Department of Materials Science and Engineering, Massachusetts Institute of Technology, Cambridge, Massachusetts, U.S.A. 02139-4307

Received May 14, 2007; Revised June 8, 2007

Abstract: Nanocomposite films were prepared by sol-gel synthesis from vanadium triisopropoxide with poly((oxyethylene)$_9$ methacrylate)-*graft*-poly(dimethyl siloxane), POEM-*g*-PDMS, producing in situ growth of vanadium oxide within the continuous ion-conducting POEM domains of microphase-separated graft copolymer. The formation of vanadium oxide was confirmed by wide angle x-ray scattering (WAXS) and Fourier transform infrared (FT-IR) spectroscopy. Small angle x-ray scattering (SAXS) revealed the spatially-selective incorporation of vanadium oxide in the POEM domains. Upon the incorporation of vanadium oxide, the domain periodicity of the graft copolymer monotonously increased from 17.2 to 21.0 nm at a vanadium content 14 v%, above which it remained almost invariant. The selective interaction of vanadium oxide with POEM was further verified by differential scanning calorimetry (DSC) and FT-IR spectroscopy. The nanocomposite films exhibited excellent mechanical properties (10^{-5}-10^{-7} dyne/cm^2), mostly due to the confinement of vanadium oxide in the POEM chains as well as the interfaces created by the microphase separation of the graft copolymer.

Keywords: nanocomposite, sol-gel, graft copolymer, microphase separation, spectroscopy.

Introduction

Organic-inorganic polymer nanocomposites have received much attention over the past decade because of their excellent properties such as electrical conductivity, mechanical toughness and catalytic activity over pristine polymer.[1-3] Especially, nanostructured polymer composites with controlled morphology have recently attracted much interest in material science. In this type of materials, microphase-separated polymers are commonly used as an efficient template to allow the access of nanoscale inorganic materials to a specific domain.[4-8] Their final morphology is determined by the cooperative organization of inorganic and organic molecular species into three-dimensionally structured arrays. In this approach, the sol-gel method as a soft chemistry is usually employed, enabling the process at a low temperature. Wiesner's groups demonstrated that the organic-inorganic hybrid materials prepared from a silicone precursor and poly(isoprene-*block*-ethylene oxide) (PI-*b*-PEO) show a versatile morphology by varying amounts of inorganic compounds.[4-6]

Vanadium oxide, e.g. V_2O_5, is a promising and attractive inorganic material for cathodes in lithium rechargeable batteries,[9-11] because it possesses a large lithium insertion capacity. It has been reported that the specific energy density of V_2O_5 is higher than that of various cathode materials such as $LiMn_2O_4$, $LiCoO_2$, and $LiNiO_2$.[12] Especially, amorphous vanadium oxide has been shown to intercalate larger amounts of lithium than the corresponding crystalline material.[13] Sometimes, electrically conductive inorganic materials such as silver or copper have been introduced to enhance its electrical conductivity and charge capacity of vanadium oxide electrode.[12-15] According to Smyrl's group,[13-15] silver-doped vanadium materials lead to improve the intercalation kinetics and rate capability of the cathodes. Much effort has been also made to produce polymer/vanadium oxide nanocomposites.[16,17] In this case, electronic conducting polymers such as polyaniline,[16] polypyrrole[17] have been used to expect the maximizing the performance of higher reversible capacity, redox cyclability, and structure stability.

Nanocomposite electrodes consisting of active inorganic compound and microphase-separated copolymer are of spe-

*Corresponding Author. E-mail: jonghak@yonsei.ac.kr

cial interest in lithium polymer batteries because they can increase the interface-to-volume ratio and thus high ion and electron transport.[18,19] Furthermore, the decrease in the relative concentration of active inorganic material will provide improved cycle life of the electrode. Recently, Mayes group demonstrated that nanocomposite anode comprising Au nanoparticles and single-walled carbon nanotubes in a block copolymer template of polyethylene oxide-based block copolymer showed a high cyclability > 600.[18]

In this study, nanocomposite films were prepared by sol-gel synthesis, producing in situ growth of vanadium oxide in a graft copolymer template. Poly((oxyethylene)$_9$ methacrylate)-*graft*-poly(dimethyl siloxane) (POEM-*g*-PDMS) was used as a templated, microphase-separated graft copolymer because it is shown to be highly ionic conductive (~10^{-5} S/cm at room temperature), mechanically strong and easily synthesized.[20] We here report on the synthesis and characterization of the templated nanocomposite films, with a highlight on interactions and nano-structural changes.

Experimental

Poly(ethylene glycol) methyl ether methacrylate monomer (M_n = 475 g/mol) and poly(dimethyl siloxane) monomethacrylate macromonomer ($M_n \approx$ 10,000 g/mol) were purchased from Aldrich. The graft copolymer with 70 : 30 wt ratio of POEM : PDMS (M_w = 86,000 g/mol, polydispersity index = 1.78) was synthesized by free radical methods, as described previously.[20-22] The nanocomposite films were prepared by sol-gel method of vanadium triisopropoxide ($VO(CHO(CH_3)_2)_3$, 99%, Alfa Aesar) with POEM-*g*-PDMS.[23] The polymer was first dissolved in acetone (5 wt%), followed by the introduction of vanadium triisopropoxide with various concentrations. To this mixture, the small amounts of water were added to maintain the mole ratio of [water] : [V] = 40 : 1. After complete stirring, the resulting sol was cast on Teflon dish and allowed to slow air dry, followed by further drying in a vacuum oven at 80 °C for two days. It should be noted that the final morphology of the nanocomposite films is strongly dependent on the speed of solvent evaporation.[23]

Wide angle x-ray scattering (WAXS) experiment was carried out on Rigaku 18kw watt rotating anode x-ray generator with CuK_α radiation (λ = 1.5406 Å) operated at 40 kV and 300 mA. The 2θ range was from 4° to 40° with a scanning speed of 3°/min and the sample to detector distance was 185 mm.

Small angle x-ray scattering (SAXS) was performed to characterize the microphase-separated structure of the nanocomposite films at 45 kV and 0.67 mA. A 600 micron x-ray beam is provided via pinhole collimation and a fine focus filament. Silver behenate with a peak at q = 1.076 nm^{-1} (or d = 5.838 nm) was used as a standard. The sample to detector distance was 1,300 mm. Two dimensional data were circularly averaged to produce $I(2\theta)$ versus 2θ plots where $I(2\theta)$ is the scattered intensity and 2θ is the scattering angle. All data were obtained using the following procedure to subtract the relevant intensity patterns/arrays: (sample-dark) - T ratio (background-dark), where T ratio is a transmission factor correction for each sample and is $(T_{sample} - T_{dark})/(T_{background} - T_{dark})$.

Thermal analysis of the nanocomposite films was conducted by differential scanning calorimeter (DSC Q100, TA Instruments, Inc.). DSC samples were heated at a rate of 20 °C/min in a flowing atmosphere of nitrogen (50 cm^3/min). The samples were encapsulated in aluminum pans tightly fitted with inverted lids to ensure good thermal contact between the sample and the pan. All data measured in this study show no difference between first and second scan.

FT-IR spectra were measured using Nicolet Magna 860 FT-IR spectrometer; 64-64 scans were signal-averaged at a resolution 4 cm^{-1}.

The dynamic mechanical properties of the nanocomposite films were probed using a strain-controlled rheometer (ARES, Rheometrics). The rheometer was operated in the parallel-plate oscillatory shear mode with a 1 mm gap at 30 °C. The sample was molded on the 25 mm diameter test fixture by pressing a film of the material to the measurement gap width. The frequency dependence of the dynamic storage and loss moduli (G' and G'', respectively) were recorded for the frequency range from 200 to 0.1 rad/s at a relatively small strain amplitude of 1.5%.

Results and Discussion

It is generally known that sol-gel synthesis from vanadium triisopropoxide precursor to vanadium oxide (i.e. V_2O_5) involves two reaction processes.[23] Initiation occurs via a hydrolysis of alkoxy ligands, producing alcohol and hydroxylated metal centers. Vanadium oxide is finally formed by a condensation reaction between -OH and -OR species. In the use of templated graft copolymer, i.e. POEM-*g*-PDMS, vanadium precursor with a high electrophilicity is expected to be selectively introduced to POEM domains with polar moiety. *In situ* growth of vanadium oxide will lead to the spatially-selective incorporation in POEM domains, maintaining the microphase-separated structure of the nanocomposite films.

To investigate the formation of vanadium oxide in templated POEM-*g*-PDMS, WAXS spectra were measured for pristine copolymer and nanocomposite films, and presented in Figure 1. Pristine POEM-*g*-PDMS (70 : 30) showed three amorphous peaks at around 8.4°, 11.9°, and 20.0°. WAXS measurements of homopolymers, i.e. PDMS and POEM, clearly reveal that the peaks at 11.9° (d-spacing = 7.4 Å) and 20.0° (4.4 Å) are originated from the chain distances of PDMS and POEM domains, respectively. Higher d-spacing value of PDMS than that of POEM is presumably due to its lower packing density, related to unusually high free vol-

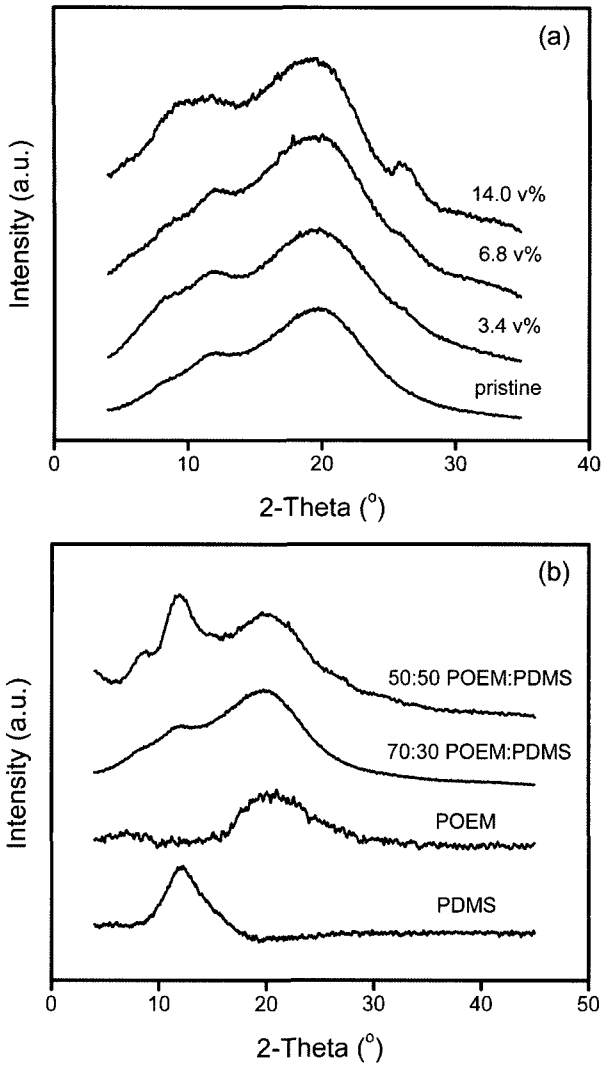

Figure 1. (a) WAXS spectra for pristine POEM-*g*-PDMS (70 : 30) and its nanocomposite films with various concentration of vanadium oxide; (b) WAXS spectra for pristine POEM-*g*-PDMS (70 : 30 and 50 : 50) and homopolymer (POEM and PDMS).

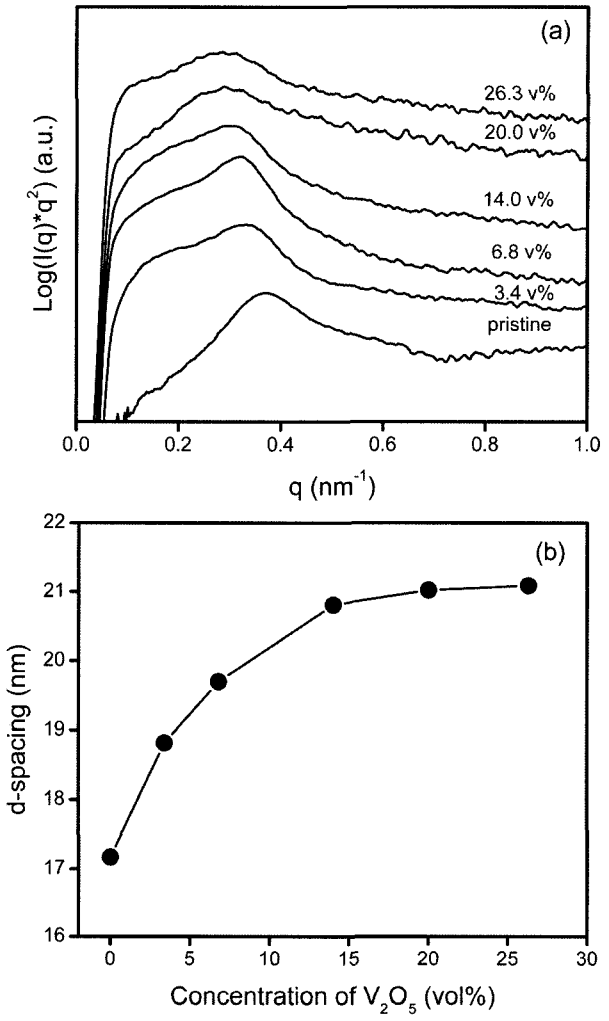

Figure 2. (a) SAXS spectra for pristine POEM-*g*-PDMS (70 : 30) and its nanocomposite films with various concentration of vanadium oxide; (b) changes in d-spacing of POEM-*g*-PDMS/V_2O_5 nanocomposite films as a function of vanadium concentration.

ume of PDMS.[24] For homopolymers with pendant groups, two amorphous peaks are usually observed in WAXS plots.[25-27] It has been demonstrated that the first peak at low 2θ reflects the interchain distance, i.e. the distance between main chains, while the second peak at high 2θ reflects the distance between inter-pendant. Thus, the weak peak at 8.4° (d spacing = 10.5 Å) for pristine graft copolymer is attributable to the distances between methacrylate main chain. Increase of PDMS portion in graft copolymers (from 70 : 30 to 50 : 50) led to the growth in the two peaks at 8.4 and 11.9° relative to the peak at 20.0°, supporting the assignment for each peak. PDMS chains are shortly dangled in methacrylate main chains and thus at high PDMS concentrations the two peaks of PDMS chains and main chains become clearly separated. The WAXS spectra for nanocomposite films with various concentration of vanadium oxide were provided in Figure 1(a). As the concentration of vanadium oxide increased, two peaks at 8.8° and 26.1°, assignable to amorphous vanadium oxide,[23] grew up, indicating the in situ formation of vanadium oxide in the templated graft copolymer.

Microphase-separated morphologies of the nanocomposites were investigated by SAXS. Figure 2(a) shows the SAXS spectra for nanocomposite films consisting of POEM-*g*-PDMS and vanadium oxide with various compositions. Pristine graft copolymer exhibited a maximum peak at q~ 0.36 nm^{-1}, suggesting its well developed, microphase-separated structure. Upon addition of vanadium oxide, the nanocomposite films remained a microphase-separated state and

their q values at maximum shifted to lower values up to 14 vol% of vanadium oxide. However, further increase of vanadium concentration did not change q value at a maximum, presenting the presence of maximum loading capacity in the templated graft copolymer. Some literatures reported that one of microdomains can be transformed into another with increasing concentrations of inorganic materials.[4-6] However, this was not observed in our system. The domain spacings of the nanocomposite films were estimated from peak maximum using Bragg relation. The variation of domain spacing in the nanocomposite films was plotted in Figure 2(b) as a function of vanadium oxide concentration. Since the concentration of POEM (70 wt%) is higher than that of PDMS (30 wt%) in POEM-*g*-PDMS, the domain spacing is assignable to the distance between isolated PDMS domains in continuous POEM domains. The domain spacings of the films monotonously increased from 17.2 to 21.0 nm with the increase of vanadium oxide up to 14 vol%, representing the spatially-selective incorporation of vanadium oxide in POEM domains.

The DSC heating curves of the pristine POEM-*g*-PDMS and its nanocomposites with vanadium oxide were presented in Figure 3(a). The pristine graft copolymer is microphase-separated, showing two T_gs at -134 and -69 °C, which can be attributed to the PDMS and POEM chains, respectively. Upon the incorporation of vanadium oxide, the T_g of PDMS remained almost invariant whereas that of POEM increased. It might be due to the fact that the vanadium oxide selectively interacts with ethylene oxide moiety of POEM domains, leading to the restricted chain mobility of POEM domains. The dependence of T_g in POEM domains on the concentration of vanadium oxide was plotted in Figure 3(b). The value of T_g monotonously increased with increasing concentration of vanadium oxide up to 14 vol%, above which it slightly decreased. This T_g behavior is consistent with the result of SAXS, demonstrating that the maximum loading capacity of POEM for vanadium oxide is 14 vol%.

The FT-IR spectra for the nanocomposite films with various concentration of vanadium oxide were measured and presented in Figure 4. The absence of -OH stretching band at around 3500-3300 cm^{-1} clearly presents that the nanocomposite films do not contain any trace of water or alcohol, commonly produced by sol-gel synthesis for the formation of vanadium oxide.[23] These by-products are considered to be removed by heating treatment at 80 °C for two days. Upon the incorporation of vanadium, the vanadyl stretching band ($\nu_{V=O}$) at 1000 cm^{-1} appears and grows up with the increase of vanadium concentration.[17,28] The intensity of this band almost linearly increased in proportion to the concen-

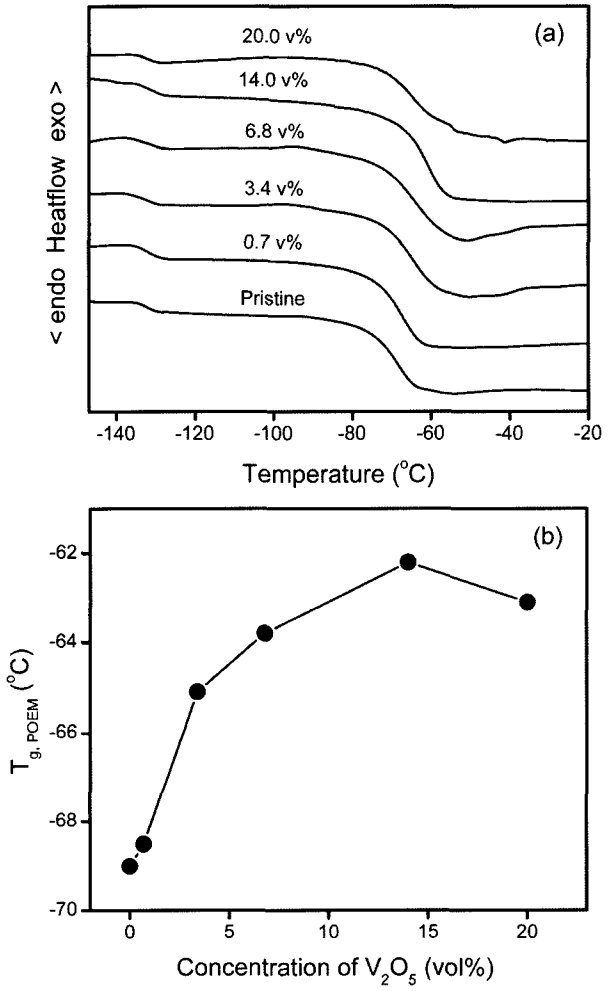

Figure 3. (a) DSC curves for pristine POEM-*g*-PDMS (70 : 30) and its nanocomposite films with various concentration of vanadium oxide; (b) changes in $T_{g,\ POEM}$ of POEM-*g*-PDMS/V_2O_5 nanocomposite films as a function of vanadium concentration.

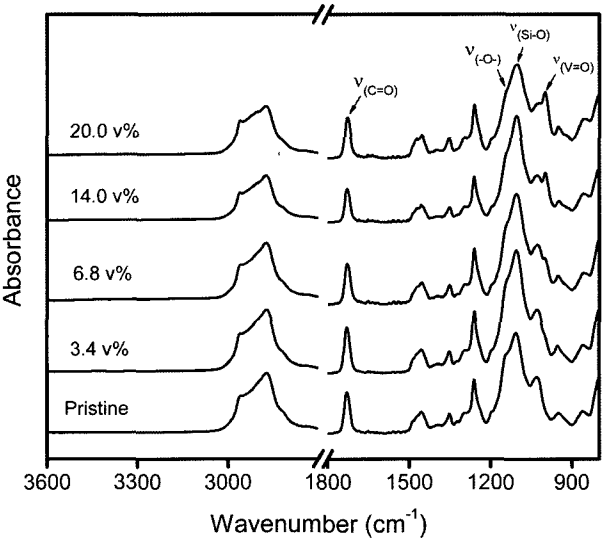

Figure 4. FT-IR spectra for pristine POEM-*g*-PDMS (70 : 30) and its nanocomposite films with various concentration of vanadium oxide.

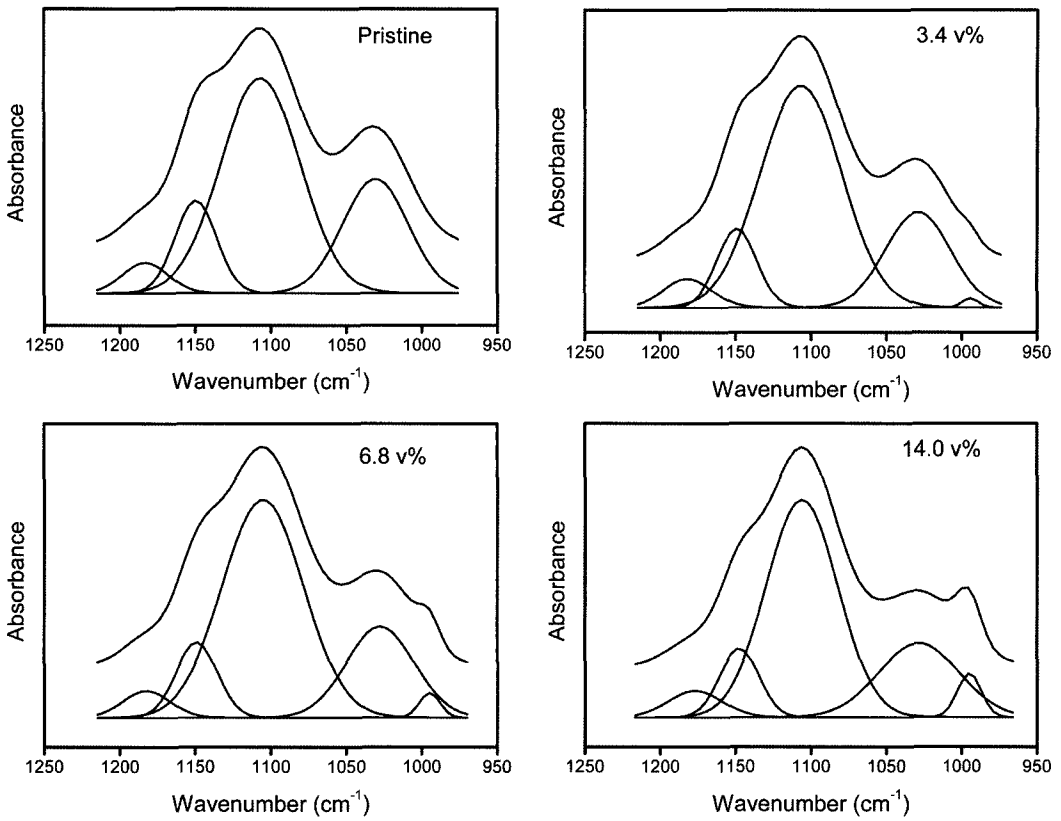

Figure 5. Deconvoluted FT-IR curves for pristine POEM-*g*-PDMS (70 : 30) and its nanocomposite films with various concentration of vanadium oxide in the range between 1250 and 950 cm^{-1}.

tration of vanadium triisopropoxide precursor, demonstrating that most of vanadium precursor participated in the reaction and converted to vanadium oxide. This high conversion yield may be attributable to the high chemical reactivity of transition metal vanadium and relatively high molar ratio of water to vanadium oxide (i.e. [water] : [V] = 40 : 1).[23] The loading of vanadium oxide resulted in the change of ether stretching band of POEM domains at 1146 cm^{-1}. It is well known that the interaction of ether oxygens with inorganic materials containing metal ions leads to the shift of free ether stretching band toward a lower wavenumber, presumably due to the loosening of the C-O bond by the electron donation.[29-31] Thus, the decrease of free ether stretching intensity at 1146 cm^{-1} is attributable to the loss of free ether oxygen by the interaction with vanadium oxide. In the mean time, ester carbonyl stretching in methacrylate at 1725 cm^{-1} remained almost invariant, representing that the electron donation ability of ester oxygen is lower than that of ether oxygen and most of vanadium oxides preferentially interact with ether oxygen among various possible coordination groups.[32] Invariant position and intensity of Si-O stretching peak at 1105 cm^{-1} also demonstrate that PDMS is not involved in specific interaction in the nanocomposites, which is known to be due to the characteristics of the Si-O bond suppressing the oxygen donor number.[33,34]

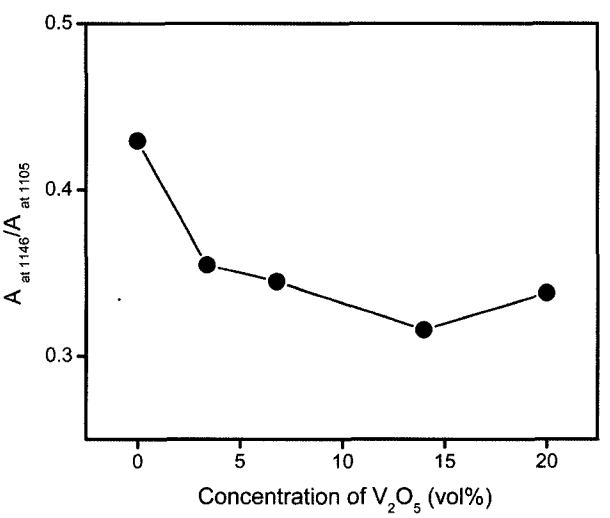

Figure 6. Changes in relative absorbance at 1146 over that at 1105 cm^{-1} for the nanocomposite films as a function of vanadium oxide concentration.

To clearly investigate the interaction of ether oxygen with vanadium oxide, the FT-IR spectra for pristine graft copoly-

mer and the nanocomposites were deconvoluted into each peak, as presented in Figure 5. Relative intensity of ether absorbance at 1146 cm^{-1} over Si-O at 1105 cm^{-1} was plotted in Figure 6 as a function of concentration of vanadium oxide. The relative intensity decreased with the increase of vanadium oxide up to 14 vol%, mostly due to the interaction of ether oxygens with vanadium. However, it abruptly increased at 20 vol%, presenting the maximum coordination capacity of ether oxygen to vanadium oxide and the partial macrophase separation of the oxide phase. This FT-IR result is consistent with those of SAXS and DSC.

Dynamic mechanical properties of nanocomposite films were investigated using rheometer. Figure 7 shows the storage (G') and loss moduli (G'') of the graft copolymer/V_2O_5 nanocomposite films as a function of reduced frequency. The microphase separation of graft-copolymer resulted in the solid-like nature of the pristine material, showing $G' > 10^5$ dyne/cm^2 and $G'' \sim \omega^{0.5}$.[20,35] The excellent mechanical property of graft copolymer originates from the interfaces created by the microphase separation between two domains. It should be noted that POEM homopolymer exhibits the low-frequency scaling behavior $G'' \sim \omega$, indicating its molten and liquid-like state.[35] Upon the addition of vanadium oxide, both the storage and loss moduli dramatically increased, due to the formation of polymer/V_2O_5 nanocomposites. It is a well-known fact that the introduction of nanoscale inorganic compounds into polymer leads to the enhancement of mechanical property in the films.[2,36] The storage modulus at a specific frequency, i.e. 0.13 rad/sec and the slope in a plot of log G'' vs log ω were plotted as a function of vanadium oxide's concentration and presented in Figure 8. It has been known that the slope is associated with the mechanical strength of the films and a lower value indicates a stronger mechanical property.[35] For example, the slope of 1 indicates

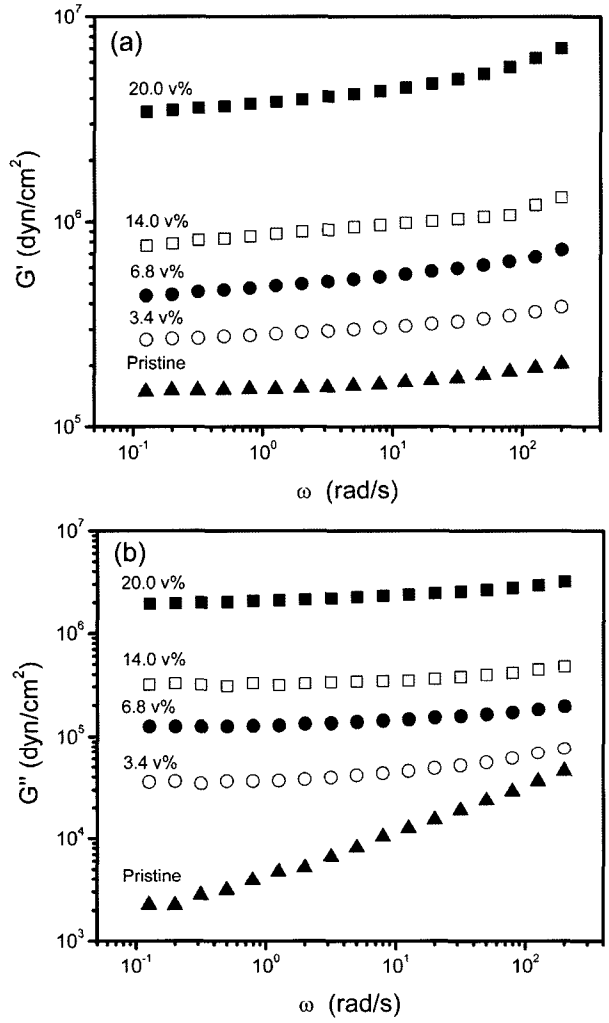

Figure 7. (a) Storage (G') and (b) loss (G'') moduli for pristine POEM-*g*-PDMS (70 : 30) and its nanocomposite films with various concentration of vanadium oxide.

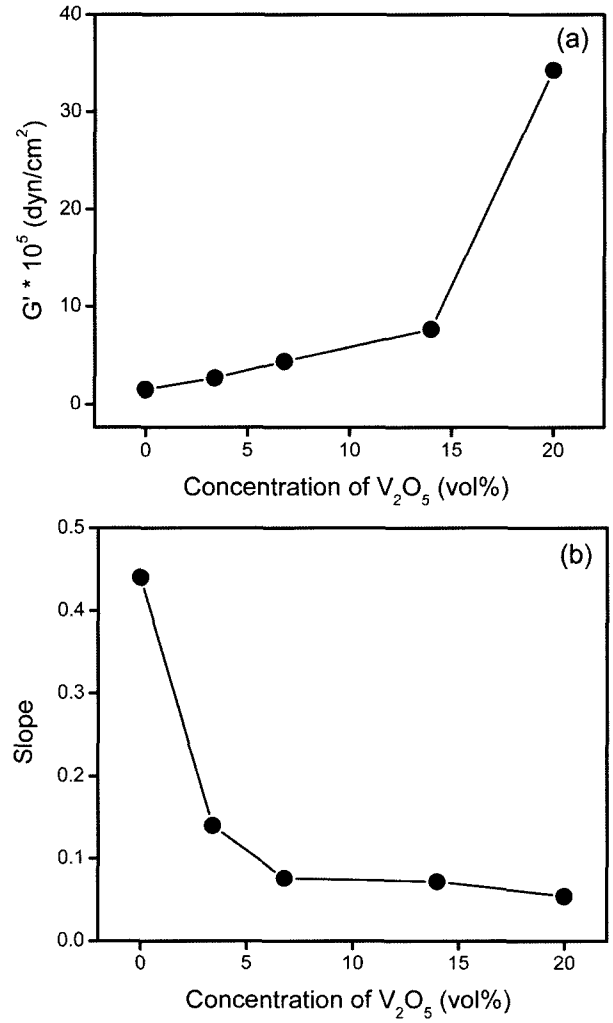

Figure 8. (a) Storage modulus (G') at 0.13 rad/sec and (b) the slope in a plot of log G'' vs log ω for nanocomposite films as a function of vanadium oxide concentration.

the molten state of polymer and 0.5 does solid nature.[35] As shown in the figure, the mechanical properties of the nanocomposite films increased with the increase of vanadium concentration, and abruptly jumped up at 20 vol% of vanadium. The significant enhancement at 20 vol% may be related to the partial macrophase separation of the oxide phase, separately forming inorganic phase with strong mechanical property. This composition is consistent with the threshold vanadium concentration for the formation of microphase-separated nanocomposite films, as confirmed by SAXS, DSC, and FT-IR spectroscopy.

Conclusions

The graft copolymer/V_2O_5 nanocomposite films were prepared using sol-gel synthesis from vanadium precursor in a microphase-separated PDSM-*g*-POEM template. WAXS and FT-IR study clearly showed that vanadium oxide was in situ grown and formed in the templated graft copolymer. The vanadium oxide was selectively incorporated in conductive POEM domains due to its specific interaction with polar ether oxygen, as confirmed by SAXS, FT-IR, and DSC. The prepared nanocomposite films exhibited enhanced mechanical properties over pristine copolymer. The graft copolymer/V_2O_5 nanocomposite films investigated in this work possesses the possible application to templated nanocomposite cathodes for lithium rechargeable batteries. Electrochemical performance of the lithium battery employing PDMS-*g*-POEM/V_2O_5 nanocomposite cathodes will be reported in the near future.

Acknowledgement. This work was supported by Korea Research Foundation Grant (KRF-2005-005-J01401).

References

(1) Y. Kwon and K. H. Kim, *Macromol. Res.*, **14**, 424 (2006).
(2) K. H. Kim, K. H. Kim, J. Huh, and W. H. Jo, *Macromol. Res.*, **15**, 178 (2007).
(3) H. S. Park, J. H. Lee, J. D. Nam, S. J. Seo, Y. K. Lee, Y. S. Oh, and H. C. Jung, *Macromol. Res.*, **14**, 430 (2006).
(4) P. F. W. Simon, R. Ulrich, H. W. Spiess, and U. Wiesner, *Chem. Mater.*, **13**, 3464 (2001).
(5) A. C. Finnefrock, R. Ulrich, G. E. S. Toombes, S. M. Gruner, and U. Wiesner, *J. Am. Chem. Soc.*, **125**, 13084 (2003).
(6) C. B. W. Garcia, Y. M. Zhang, S. Mahajan, F. DiSalvo, and U. Wiesner, *J. Am. Chem. Soc.*, **125**, 13310 (2003).
(7) E. A. Olivetti, J. H. Kim, D. R. Sadoway, A. Asatekin, and A. M. Mayes, *Chem. Mater.*, **18**, 2828 (2006).
(8) K. A. Mauritz, R. I. Blackwell, and F. L. Beyer, *Polymer*, **45**, 3001 (2004).
(9) B. Y. Huang, C. C. Cook, S. Mui, P. P. Soo, D. H. Staelin, A. M. Mayes, and D. R. Sadoway, *J. Power Source*, **97**, 674 (2001).
(10) P. E. Trapa, B. Y. Huang, Y. Y. Won, D. R. Sadoway, and A. M. Mayes, *Electrochem. Solid State Lett.*, **5**, A85 (2002).
(11) A. Mantoux, H. Groult, E. Balnois, P. Doppelt, and L. Guerroudji, *J. Electrochem. Soc.*, **151**, A368 (2004).
(12) Y.-Q. Chu and Q.-Z. Qin, *Chem. Mater.*, **14**, 3152 (2002).
(13) F. Coustier, S. Passerini, and W. H. Smyrl, *Solid State Ionics*, **100**, 247 (1997).
(14) F. Coustier, J. Hill, B. B. Owens, S. Passerini, and W. H. Smyrl, *J. Electrochem. Soc.*, **146**, 1355 (1999).
(15) B. B. Owens, S. Passerini, and W. H. Smyrl, *Electrochim. Acta*, **45**, 215 (1999).
(16) Z. F. Li and E. Ruckenstein, *Langmuir*, **18**, 6956 (2002).
(17) J. Harreld, H. P. Wong, B. C. Dave, B. Dunn, and L. F. Nazar, *J. Non-Cryst. Solids*, **225**, 319 (1998).
(18) S. C. Mui, P. E. Trapa, B. Huang, P. P. Soo, M. I. Lozow, T. C. Wang, R. E. Cohen, A. N. Mansour, S. Mukerjee, A. M. Mayes, and D. R. Sadoway, *J. Electrochem. Soc.*, **149**, A1610 (2002).
(19) S. E. Bullock and P. Kofinas, *J. Power Sources*, **132**, 256 (2004).
(20) P. E. Trapa, Y.-Y. Won, S. C. Mui, E. A. Olivetti, B. H. Huang, D. R. Sadoway, A. M. Mayes, and S. Dallek, *J. Electrochem. Soc.*, **152**, A1 (2005).
(21) D. K. Lee, K. J. Lee, Y. W. Kim, B. R. Min, and J. H. Kim, *J. Polym. Sci.; Part B: Polym. Phys.*, **45**, 1018 (2007).
(22) Y. W. Kim, D. K. Lee, K. J. Lee, B. R. Min, and J. H. Kim, *J. Polym. Sci.; Part B: Polym. Phys.*, **45**, 1283 (2007).
(23) G. Sudant, E. Baudrin, B. Dunn, and J.-M. Tarascon, *J. Electrochem. Soc.*, **151**, A666 (2004).
(24) T. C. Merkel, R. P. Gupta, B. S. Turk, and B. C. Freeman, *J. Membr. Sci.*, **191**, 85 (2001).
(25) M. Aguilar-Vega and D. R. Paul, *J. Polym. Sci. B*, **31**, 1577 (1993).
(26) J. H. Kim, B. R. Min, C. K. Kim, J. Won, and Y. S. Kang, *Macromolecules*, **35**, 5250 (2002).
(27) J. H. Kim, J. Won, and Y. S. Kang, *J. Polym. Sci.; Part B: Polym. Phys.*, **42**, 2263 (2004).
(28) C.-G. Wu, D. C. DeGroot, H. O. Marcy, J. L. Schindler, C. R. Kannewurf, Y.-J. Liu, W. Hirpo, and M. G. Kanatzidis, *Chem. Mater.*, **8**, 1992 (1996).
(29) D. Swierczynski, A. Zalewska, and W. Wieczorek, *Chem. Mater.*, **13**, 1560 (2001).
(30) J. H. Kim, B. R. Min, K. B. Lee, J. Won, and Y. S. Kang, *Chem. Commun.*, 2732 (2002).
(31) J. H. Kim, B. R. Min, C. K. Kim, J. Won, and Y. S. Kang, *J. Phys. Chem. B*, **106**, 2786 (2002).
(32) J. H. Kim, B. R. Min, J. Won, S. H. Joo, H. S. Kim, and Y. S. Kang, *Macromolecules*, **36**, 6183 (2003).
(33) J. R. MacCallum and C. A. Vincent, *Polymer Electrolyte Reviews*, Elsevier Applied Science, London and New York, 1987, p 91.
(34) J. H. Kim, J. Won, and Y. S. Kang, *J. Membr. Sci.*, **241**, 403 (2004).
(35) A.-V. G. Ruzette, P. P. Soo, D. R. Sadoway, and A. M. Mayes, *J. Electrochem. Soc.*, **148**, A537 (2001).
(36) H. M. Jeong, M. Y. Choi, M. S. Kim, J. H. An, J. S. Jung, J. H. Kim, B. K. Kim, and S. M. Cho, *Macromol. Res.*, **14**, 610 (2006).